Phase formation and ground state properties of $CeCo_9Si_4$

2010 J. Phys.: Condens. Matter 22 135601

(http://iopscience.iop.org/0953-8984/22/13/135601)

J. Phys.: Condens. Matter **22** (2010) 135601 (7pp) doi:10.1088/0953-8984/22/13/135601

Phase formation and ground state properties of $CeCo_9Si_4$

M Giovannini[1,2], M Hadwig[3], R Pasero[1], E Bauer[3], G Hilscher[3], M Reissner[3], P Rogl[4] and H Michor[3,5]

[1] Dipartimento di Chimica e Chimica Industriale, Università di Genova, Via Dodecaneso 31, I-16146 Genova, Italy
[2] CNR-SPIN, Corso Perrone 24, I-16152 Genova, Italy
[3] Institut für Festkörperphysik, T.U. Wien, Wiedner Hauptstrasse 8–10, A-1040 Wien, Austria
[4] Institut für Physikalische Chemie, Universität Wien, Währingerstrasse 42, A-1090 Wien, Austria

E-mail: michor@ifp.tuwien.ac.at

Received 14 December 2009, in final form 5 February 2010
Published 12 March 2010
Online at stacks.iop.org/JPhysCM/22/135601

Abstract
The phase relations of the $CeCo_{9+\delta}Si_{4-\delta}$ system have been studied by means of scanning electron microscopy, electron microprobe analysis and x-ray diffraction. Essentially single phase samples $CeCo_{9+\delta}Si_{4-\delta}$ (structure-type $LaFe_9Si_4$ with space group $I4/mcm$) are formed in a narrow composition range $-0.3 \leqslant \delta < 0.1$, where stoichiometric $CeCo_9Si_4$ exhibits full structural order in space group $I4/mcm$. The evolution of the ground state of correlated 3d and 4f electrons in the solid solution $CeCo_{9+\delta}Si_{4-\delta}$ has been investigated by dc susceptibility, magnetization, specific heat and resistivity measurements. Stoichiometric $CeCo_9Si_4$ exhibits paramagnetic Kondo lattice behaviour with a largely reduced Co 3d contribution to the magnetic susceptibility as compared to nearly ferromagnetic $LaCo_9Si_4$. Nonetheless, very similar to the solid solution $LaCo_{9+\delta}Si_{4-\delta}$, weak ferromagnetism is observed in $CeCo_{9+\delta}Si_{4-\delta}$ for $\delta > 0$ and is attributed to substitutional disorder at the Si-sublattice.

(Some figures in this article are in colour only in the electronic version)

1. Introduction

Compounds RT_9X_4 (R = rare earth, T = 3d transition metal and X = p-block elements) crystallizing in an ordered tetragonal variant of the cubic $NaZn_{13}$-type (see e.g. [1, 2]) have attracted interest because they reveal a wide spectrum of ground state features. These comprise, for example, strong electronic correlations like in $CeNi_9X_4$ (X = Si and Ge) showing Kondo lattice behaviour [3] as well as heavy fermion non-Fermi liquid behaviour [4, 5]. Additionally there is itinerant magnetism of 3d electrons in RCo_9Si_4, including weak itinerant ferromagnetism in YCo_9Si_4 [6], ferrimagnetism in $GdCo_9Si_4$ [7] and, most interestingly, strongly exchange enhanced Pauli paramagnetism and itinerant electron metamagnetism in $LaCo_9Si_4$ [8]. In the specific case of $CeCo_9Si_4$, where both 4f and 3d electrons are involved in the formation of a ground state of strongly correlated electrons, our previous studies revealed intermediate valence behaviour of Ce, causing a paramagnetic ground state in $CeCo_9Si_4$ with a rather weak cobalt sublattice contribution as compared with other RCo_9Si_4 compounds [9, 10]. As cobalt itinerant magnetism has been reported to be very sensitive to the Co–Si stoichiometry in the solid solution $LaCo_{13-x}Si_x$, in particular near the critical composition $x = 4$ [11, 12], we explored the Co/Si solid solubility in $CeCo_{9+\delta}Si_{4-\delta}$ and studied the composition dependence of magnetic and electronic properties.

In this paper we report on a crystallographic characterization of the fully ordered ternary compound $CeCo_9Si_4$ and analyse the sublattice disorder in the solid solution $CeCo_{9+\delta}Si_{4-\delta}$. The evolution of the electronic ground state and its relation to the Co/Si substitution at specific crystallographic sublattices is discussed by means of magnetization, specific heat and resistivity measurements.

2. Experimental details

Polycrystalline samples of $CeCo_{13-x}Si_x$ with nominal compositions varying from $CeCo_{10}Si_3$ to $CeCo_8Si_5$ were prepared

[5] Author to whom any correspondence should be addressed.

Table 1. Results obtained from an EMPA investigation of samples with nominal compositions $CeCo_{13-x}Si_x$; s.s. = Co/Si solid solution.

x	Phases present	Phase comp. (at.% Ce–Co–Si)	Comments
3.0	bct 1:13	7–67–26	Majority phase
	Ce_2Co_{17} s.s.	12–71–17	
	bct 1:11	8–74–18	
3.6	bct 1:13	7–66–27	
	Ce_2Co_{17} s.s.	12–71–17	Minor phase
3.9	bct 1:13	7–64–29	
	Ce_2Co_{17} s.s.	12–71–17	Traces
3.95	bct 1:13	7–63–30	
3.98	bct 1:13	7–63–30	
4.0	bct 1:13	7–63–30	
4.02	bct 1:13	7–63–30	
4.1	bct 1:13	7–62–31	
	$CeCo_2Si_2$	20–39–41	Traces
4.3	bct 1:13	7–61–32	
	$CeCo_2Si_2$	20–39–41	Minor phase
4.5	bct 1:13	7–60–33	Majority phase
	$CeCo_2Si_2$	20–39–41	
	Co_2Si	0–65–35	
5.0	bct 1:13	7–56–37	Majority phase
	$CeCo_2Si_2$	20–39–41	
	Co_2Si	0–65–35	

by high frequency induction melting. The starting materials, cerium ingots (Ames MPC [13], 99.95%), cobalt ingots (Umicore, 99.999%) and silicon chips (Alpha Aesar, 99.9999%), were melted together in a two-step procedure: (i) Cobalt and silicon were melted together four times. (ii) The required amounts of Ce were melted together with the precursor CoSi-alloys. To ensure homogeneity, the buttons were broken, flipped over and melted several times, and finally sealed in an evacuated quartz tube and annealed at 1050 °C for 1 week. Samples were prepared with 0.01–0.02 f.u. cerium in excess to prohibit their contamination with traces of the ferromagnetic impurity phase $Co_{0.92}Si_{\sim 0.08}$ (see details in section 3).

In order to examine the phase formation of $CeCo_{13-x}Si_x$ and the corresponding homogeneity regions we investigated selected samples by scanning electron microscopy (SEM) and electron microprobe analysis (EMPA) based on energy dispersive x-ray spectroscopy.

Temperature dependent electrical resistivity measurements were performed in a He-bath cryostat (2–300 K) and for selected samples in a ^{3}He-cryostat (0.4–300 K) on bar-shaped samples applying a standard four-probe dc method with gold pins as voltage and current contacts. The dc susceptibility/magnetization measurements were performed in a 6 T SQUID magnetometer and a 9 T vibrating sample magnetometer (VSM). Specific heat measurements were carried out on samples of about 1 g in the temperature range 2–140 K employing an adiabatic step heating technique.

3. Phase formation and crystal structure

The EMPA results for the polycrystalline samples prepared along the composition line $CeCo_{13-x}Si_x$ ($3.0 < x < 5.0$) are summarized in table 1. EMPA and x-ray diffraction studies reveal the presence of two branches in the ternary phase diagram with Co/Si solid solutions slightly shifted in Ce composition: the body centred tetragonal (bct) phase 1:13, $LaFe_9Si_4$-type and the bct 1:11, $BaCd_{11}$-type. Similar results were reported for $GdCo_{13-x}Si_x$ [7].

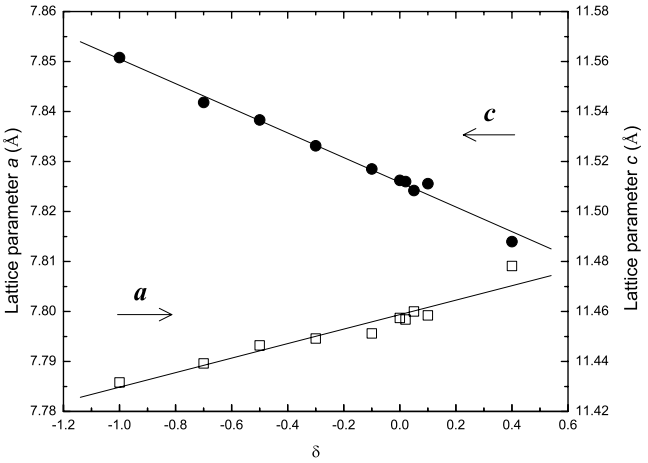

Figure 1. Tetragonal lattice parameters a (empty squares) and c (full circles) versus the composition parameter δ of $CeCo_{9+\delta}Si_{4-\delta}$.

The bct 1:13 phase forms in a composition range $CeCo_{9.4}Si_{3.6}$ to $CeCo_8Si_5$, as evidenced by the phase composition and the trend of the lattice parameters (see table 1 and figure 1). The alloys outside the range $CeCo_{9.1}Si_{3.9}$ to $CeCo_{8.7}Si_{4.3}$, however, are not single phase and the bct 1:13 phase is present together with other minority phases. The values of the lattice parameters of the phase 1:13, as a function of the composition parameter δ of $CeCo_{9+\delta}Si_{4-\delta}$, are displayed in figure 1. Whereas the lattice parameter c decreases linearly with increasing δ, the opposite trend is observed for the lattice parameter a. These trends are very similar to those reported for the analogous systems $LaCo_{9+\delta}Si_{4-\delta}$ [12] and $GdCo_{9+\delta}Si_{4-\delta}$ [14]. Furthermore, the values of the lattice parameters $a = 7.7889$ Å and $c = 11.5273$ Å obtained by Moze *et al* [15] for $Ce_2Co_{17}Si_9$ (corresponding to the composition point $\delta = -0.5$) and those determined earlier [12] for $CeCo_9Si_4$ ($a = 7.801$ Å, $c = 11.521$ Å) are in reasonable agreement with the trend depicted in figure 1.

Room temperature structure investigation of $CeCo_9Si_4$ has been performed on a small single crystal ($80 \times 50 \times 50$ μm^3) on a four-circle Nonius Kappa diffractometer equipped with a CCD area detector. For the structure refinement we used 410 reflections $>4\sigma(F_0)$ out of 475. All details of the applied methodology were recently summarized in the context of our structure investigation on Ce- and $LaNi_9Si_4$ [3]. Analogous to $LaNi_9Si_4$ and $LaCo_9Si_4$, single crystal x-ray diffraction reveals, for stoichiometric $CeCo_9Si_4$, a fully ordered tetragonal $LaFe_9Si_4$-type structure [2] ($NaZn_{13}$-derivative with space group $I4/mcm$) as depicted in figure 2. The occupancies of all crystallographic sites have been refined but did not reveal any significant deviations from stoichiometry. Refining anisotropic thermal displacement factors in the final run yielded R-values as low as 0.023 (GOF = 1.083) confirming the structural model with full atomic order. The results of the structure determination are summarized in table 2.

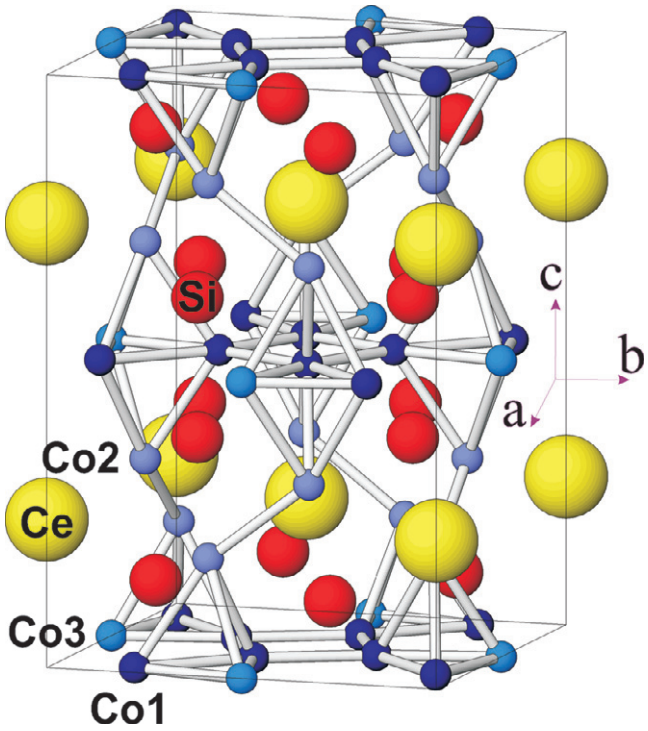

Figure 2. Crystal structure of $CeCo_9Si_4$.

Table 2. X-ray single crystal data for $CeCo_9Si_4$; space group $I4/mcm$; no. 140.

Atom	Wyckoff p.	Coordinates
	$a = 7.8014(2)$ Å; $c = 11.5206(4)$ Å	
Ce	4a	$(0, 0, \frac{1}{4})$
Co(1)	16k	$(x, y, 0)$ $x = 0.069\,69(6)$; $y = 0.200\,41(6)$
Co(2)	$16l_1$	$(x, x + \frac{1}{2}, z)$ $x = 0.628\,43(4)$; $z = 0.180\,61(5)$
Co(3)	4d	$(0, \frac{1}{2}, 0)$
Si	$16l_2$	$(x, x + \frac{1}{2}, z)$ $x = 0.170\,15(9)$; $z = 0.120\,87(9)$

Rietveld refinements of powder x-ray diffraction data of the off-stoichiometric samples $CeCo_{9.4}Si_{3.6}$ and $CeCo_{8.7}Si_{4.3}$ were carried out. The observed and calculated diffraction pattern for the two compounds are depicted in figures 3 and 4, respectively. Tables 3 and 4 summarize the results of Rietveld refinements of powder x-ray diffraction data for the two off-stoichiometric samples. The secondary phases detected by SEM analyses (see table 1) were included in the refinements in order to obtain indications of the weight fractions, although their peaks are very small (see tables 3 and 4).

Starting from the ordered compound, which corresponds to $CeCo_{9+\delta}Si_{4-\delta}$ with $\delta = 0$ and with Si saturating the site $16l_2$, in the range $\delta > 0$ some Co atoms are expected to replace Si atoms at the same site $16l_2$. This assumption is corroborated by the results of our Rietveld refinement of powder x-ray diffraction data for $CeCo_{9.4}Si_{3.6}$ (see table 3 and figure 3). Similar results for the structural properties of Co-rich samples

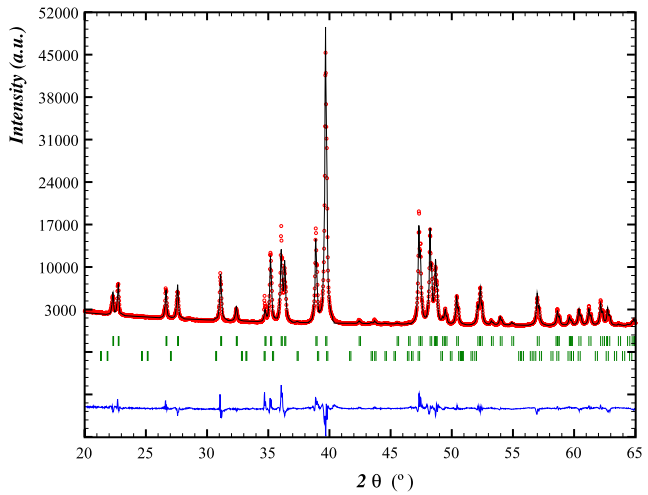

Figure 3. Part of the experimental x-ray diffraction pattern of $CeCo_{9.4}Si_{3.6}$ resulting from Rietveld refinement. The experimental data are shown by the symbols, while the line through the data represents the calculated diffractogram. The lower curve is the difference curve. The ticks indicate the 2θ values of Bragg peaks of bct 1:13 and Ce_2Co_{17} (below).

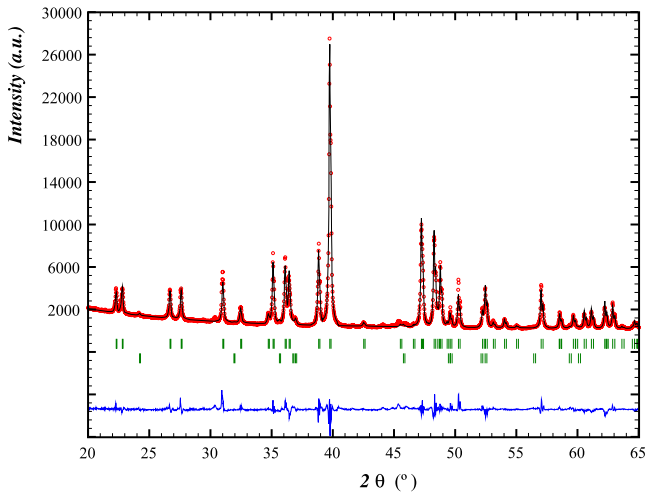

Figure 4. Part of the experimental x-ray diffraction pattern of $CeCo_{8.7}Si_{4.3}$ resulting from Rietveld refinement. The experimental data are shown by the symbols, while the line through the data represents the calculated diffractogram. The lower curve is the difference curve. The ticks indicate the 2θ values of Bragg peaks of bct 1:13 and $CeCo_2Si_2$ (below).

of the solid solution $GdCo_{13-x}Si_x$ were reported by Heiba *et al* [14].

On the other hand, in the range $\delta < 0$, excess Si atoms with respect to the ordered compound $CeCo_9Si_4$ are not distributed randomly over the available crystallographic sites, but share mainly the 16k site with Co (i.e. the Co1 site in figure 2) as noted earlier by Moze *et al* in the case of the sample with nominal composition $Ce_2Co_{17}Si_9$ [15]. In fact, in our Rietveld refinement (see table 4 and figure 4) the occupancies of the other crystallographic sites of Co ($16l_1$ and 4d which are Co2 and Co3 in figure 2) were refined with respect to Co/Si replacements but no significant deviations from full Co occupancies were revealed.

Table 3. Rietveld refinement results for $CeCo_{9.4}Si_{3.6}$: space group $I4/mcm$; no. 140. 'Occ.' = occupation in %; residual values: $R_B = 0.0728$, $R_F = 0.0522$, $R_{WP} = 0.102$, weight fraction of $Ce_2Co_{17} = 2\%$.

Atom	Wyckoff p.	Coordinates	Occ.
$a = 7.8124(1)$ Å; $c = 11.4915(2)$ Å			
Ce	4a	$(0, 0, \frac{1}{4})$	100
Co(1)	16k	$(x, y, 0)$	100
		$x = 0.0662(1)$; $y = 0.1999(1)$	
Co(2)	$16l_1$	$(x, x + \frac{1}{2}, z)$	100
		$x = 0.6276(1)$; $z = 0.1809(1)$	
Co(3)	4d	$(0, \frac{1}{2}, 0)$	100
Si(1)	$16l_2$	$(x, x + \frac{1}{2}, z)$	92
Co(4)	$16l_2$	$(x, x + \frac{1}{2}, z)$	8
		$x = 0.1737(2)$; $z = 0.1197(2)$	

Table 4. Rietveld refinement results for $CeCo_{8.7}Si_{4.3}$: space group $I4/mcm$; no. 140. 'Occ.' = occupation in %; residual values: $R_B = 0.0838$, $R_F = 0.0681$, $R_{WP} = 0.128$, weight fraction of $CeCo_2Si_2 = 3\%$.

Atom	Wyckoff p.	Coordinates	Occ.
$a = 7.7941(2)$ Å; $c = 11.5272(2)$ Å			
Ce	4a	$(0, 0, \frac{1}{4})$	100
Co(1)	16k	$(x, y, 0)$	93.6
Si(1)	16k	$(x, y, 0)$	6.4
		$x = 0.0705(1)$; $y = 0.1996(1)$	
Co(2)	$16l_1$	$(x, x + \frac{1}{2}, z)$	100
		$x = 0.6277(1)$; $z = 0.1891(1)$	
Co(3)	4d	$(0, \frac{1}{2}, 0)$	100
Si(2)	$16l_2$	$(x, x + \frac{1}{2}, z)$	100
		$x = 0.1696(2)$; $z = 0.1225(2)$	

The composition at $\delta = 0$, i.e. stoichiometric $CeCo_9Si_4$, is then at the crossover between two kinds of disordered sublattices and consequently, moving along the solid solution through this point, a change in the physical properties of the ground state can be expected (see next sections).

4. Evolution of magnetic and electronic properties in $CeCo_{9+\delta}Si_{4-\delta}$

4.1. Experiment

Magnetic, thermodynamic and transport properties of $CeCo_9Si_4$ and related samples $CeCo_{9+\delta}Si_{4-\delta}$ with compositions $-0.3 \leqslant \delta < 0.1$ (i.e. the essentially single phase samples located well within the limits of solid solubility of the $LaFe_9Si_4$ structure-type) were investigated with respect to the magnetic ground state resulting from 4f and 3d correlated electrons. These results are compared with earlier studies on the ground state properties of the related isostructural solid solution $LaCo_{9+\delta}Si_{4-\delta}$ with an empty 4f shell. The latter system exhibits weak ferromagnetism for $\delta > 0$, itinerant electron metamagnetism for $\delta = 0$ and exchange enhanced Pauli paramagnetism for $\delta \leqslant 0$ [8, 12].

Low temperature isothermal magnetization measurements of $CeCo_{9+\delta}Si_{4-\delta}$ at 2 K, are displayed as $M(H)$ in figures 5(a) and (b) and as Arrott plots, M^2 versus H/M, in figures 5(c) and (d) for Si-rich ($\delta \leqslant 0$) and Co-rich ($\delta \geqslant 0$) samples, respectively.

For $CeCo_9Si_4$ and Si-rich samples, $M(H)$ data in figure 5(a) and corresponding Arrott plots in figure 5(c) reveal a paramagnetic ground state which is corroborated by the temperature dependent magnetic susceptibilities of these Si-rich samples, $\chi(T) \equiv M(T)/H$, measured at 1 T shown in figure 6(a). The analysis of the paramagnetic susceptibilities $\chi(T)$ in terms of a temperature independent Pauli susceptibility χ_0 plus a Curie–Weiss contribution

$$\chi(T) = \chi_0 + \frac{C}{T - \Theta} \tag{1}$$

yields a rather composition independent $\chi_0 \simeq 5$–6×10^{-3} emu mol^{-1} for $CeCo_9Si_4$ and Si-rich samples, but a significant variation of the Curie constants ranging from $C = 1.44$ emu K mol^{-1} for $CeCo_9Si_4$ to $C = 0.55$ emu K mol^{-1} for $CeCo_{8.7}Si_{4.3}$ and paramagnetic Curie temperatures ranging from $\Theta = -27$ K ($CeCo_{8.98}Si_{4.02}$) to $\Theta = -114$ K ($CeCo_4Si_4$) and finally $\Theta \simeq -600$ K for $CeCo_{8.7}Si_{4.3}$. The corresponding effective paramagnetic moments μ_{eff} of 3.4 μ_B/f.u. ($CeCo_9Si_4$) to 1.77 μ_B/f.u. ($CeCo_{8.7}Si_{4.3}$) are smaller than that of the isostructural compound $LaCo_9Si_4$ with empty 4f states. The latter exhibits a high temperature effective Co moment per formula unit, $\mu_{eff} \simeq 3.58$ μ_B/f.u., and a positive $\Theta \simeq +28$ K [7]. The negative paramagnetic Curie temperatures of $CeCo_9Si_4$ and Si-rich $CeCo_{9+\delta}Si_{4-\delta}$ samples are attributed to a weakening and over-compensation of ferromagnetic correlations in the 3d band by the strong Kondo coupling revealed by high-energy electron spectroscopy [10] (see section 4.2 for further discussion).

The substitution of cobalt by silicon is expected to weaken the exchange enhancement of the 3d magnetic susceptibility, and indeed for $CeCo_{8.9}Si_{4.3}$ the absolute value of the low temperature susceptibility, $\chi(2\text{ K}) \simeq 10 \times 10^{-3}$ emu mol^{-1}, is clearly reduced as compared to $CeCo_9Si_4$ with $\chi(2\text{ K}) \simeq 17 \times 10^{-3}$ emu mol^{-1}. $CeCo_{8.98}Si_{4.02}$ and $CeCo_{8.9}Si_{4.1}$, however, exhibit slightly larger susceptibilities than stoichiometric $CeCo_9Si_4$. In particular in the case of $CeCo_{8.98}Si_{4.02}$, with tiny off-stoichiometry towards the Si-rich side, substitutional disorder pushes the ground state initially closer towards ferromagnetism (see Arrott plots in figure 5(c)).

The weakly temperature dependent Pauli-like shape of the susceptibility of $CeCo_9Si_4$ and especially $CeCo_{8.9}Si_{4.3}$ (see $\chi(T)$ in figure 6(a)) clearly indicates an intermediate valence of the Ce 4f states, i.e. strong Kondo screening of the Ce 4f moments.

For all Co-rich samples, $CeCo_{9+\delta}Si_{4-\delta}$ with $\delta > 0$, spontaneous ferromagnetic order is revealed by the 2 K isothermal magnetization $M(H)$ shown in figure 5(b) and the corresponding Arrott plots in figure 5(d). For the sake of clarity of the Arrott plots, all $M(H)$ measurements were carried out subsequent to field cooling in typically 0.1 T to avoid the domain processes at fields below 1 T. Similar composition dependent magnetic properties were reported for $LaCo_{9+\delta}Si_{4-\delta}$ where weak ferromagnetism appears for

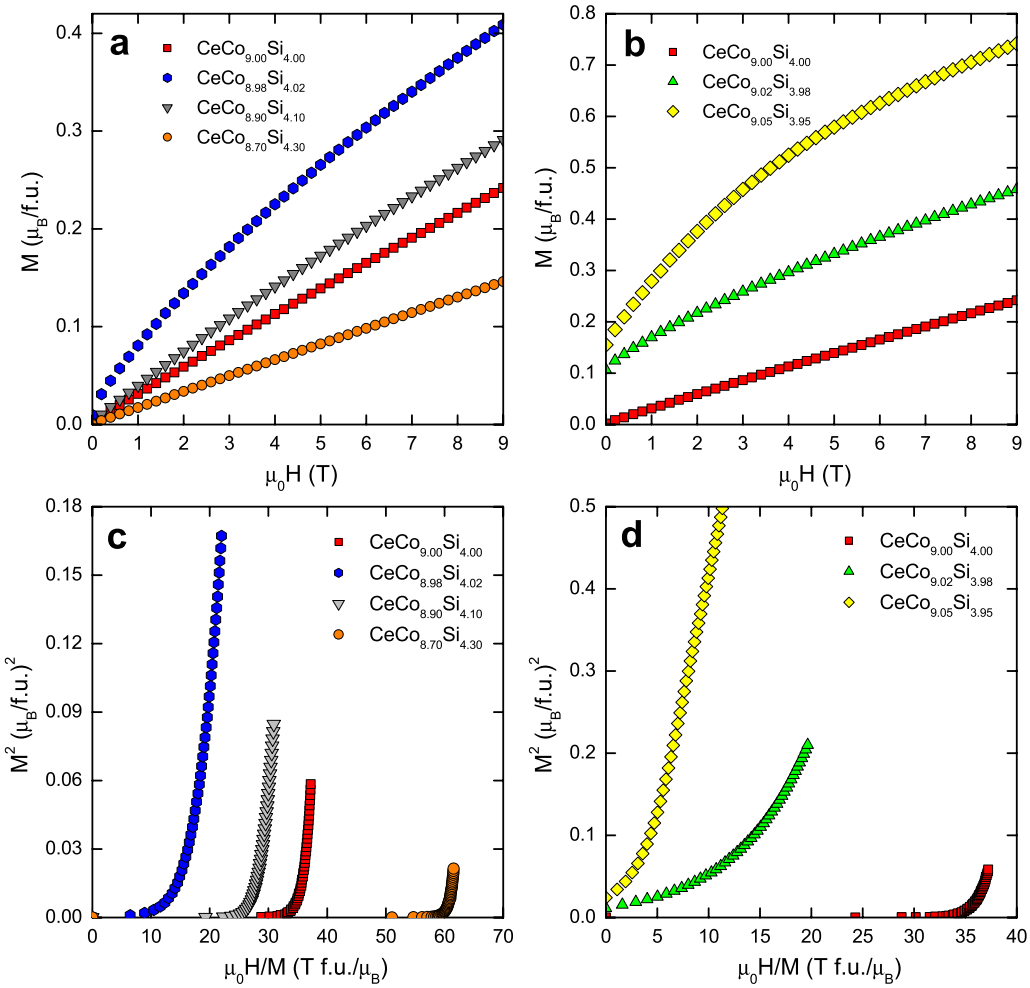

Figure 5. Isothermal magnetization $M(H)$ of $CeCo_{9+\delta}Si_{4-\delta}$ at 2 K with Si-rich composition (a) and Co-rich composition (b) and corresponding Arrott plots M^2 versus H/M of Si-rich (c) and Co-rich compositions (d).

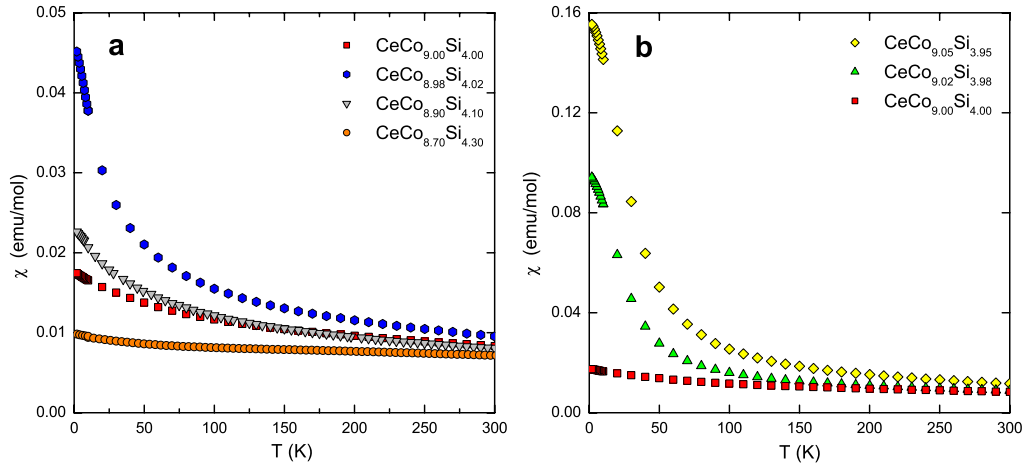

Figure 6. Temperature dependent magnetic susceptibility $\chi \equiv M/H$ measured at 1 T for $CeCo_{9+\delta}Si_{4-\delta}$ with $\delta \leqslant 0$ in (a) and $\delta \geqslant 0$ in (b).

$\delta > 0$. The Curie temperatures T_C derived from the temperature dependent susceptibilities (see figure 6(b)) and more precisely from the temperature dependence of the remanent magnetization observed in $M(H)$ measurements (not shown) are about 20 K for $CeCo_{9.02}Si_{3.98}$ and about 30 K for $CeCo_{9.05}Si_{3.95}$. These Curie temperatures are of comparable magnitude to those of corresponding compositions $LaCo_{9+\delta}Si_{4-\delta}$, but with less sharply defined transitions in the Ce system where intermediate valence of the 4f states may amplify the effect of substitutional disorder at the Si-16l sites.

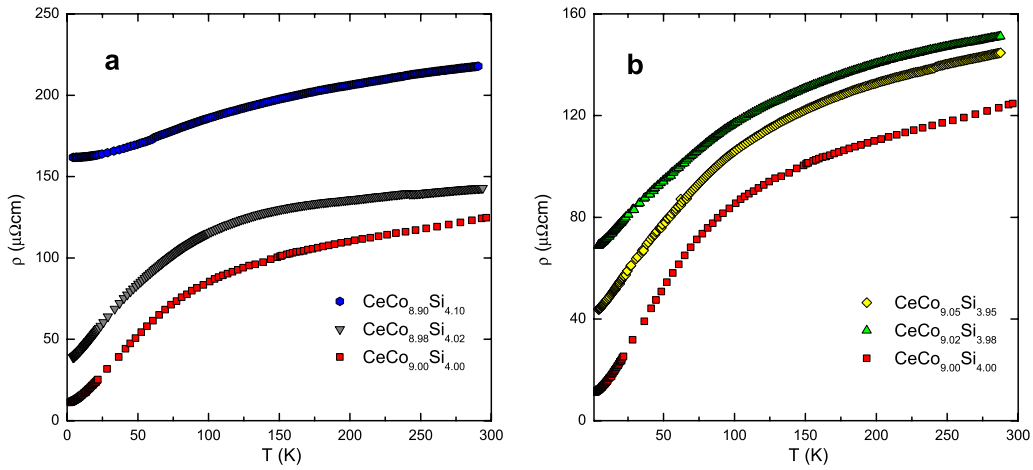

Figure 7. Temperature dependent resistivity $\rho(T)$ of $CeCo_{9+\delta}Si_{4-\delta}$ with $\delta \leqslant 0$, i.e. Si-rich (a) and $\delta \geqslant 0$, i.e. Co-rich (b).

The Arrott plot in figure 5(d) reveals an increase in the ordered moment from 0.11 μ_B/f.u. in the case of $CeCo_{9.02}Si_{3.98}$ to about 0.16 μ_B/f.u. for $CeCo_{9.05}Si_{3.95}$.

The temperature dependent electrical resistivity, $\rho(T)$, of $CeCo_{9+\delta}Si_{4-\delta}$ is shown in figures 7(a) and (b) for Si-rich ($\delta \leqslant 0$) and Co-rich ($\delta \geqslant 0$) compositions, respectively. For the stoichiometric composition $CeCo_9Si_4$ single crystal XRD reveals a fully ordered arrangement of Ce, Co and Si atoms in the space group $I4/mcm$ (see section 3), thus taking an exceptional position in the solid solution $CeCo_{9+\delta}Si_{4-\delta}$. The reduction of crystallographic order for all compositions with $\delta \neq 0$ is clearly indicated by the significant increase of the residual resistivity ρ_0 as compared to $\rho_0 \sim 10$ $\mu\Omega$ cm of stoichiometric $CeCo_9Si_4$. Even tiny off-stoichiometry, e.g. $\delta = -0.02$ with just 0.05 at.% Co replaced by Si at 16l sites, increases ρ_0 to above 40 $\mu\Omega$ cm. Similar trends of $\rho_0(\delta)$ were also observed for solid solutions $GdCo_{9+\delta}Si_{4-\delta}$ [7] and $LaCo_{9+\delta}Si_{4-\delta}$ [12]. Below 4 K the temperature dependent resistivity of stoichiometric $CeCo_9Si_4$ exhibits Fermi liquid behaviour, $\rho(T) = \rho_0 + AT^2$ with $A \simeq 0.046$ $\mu\Omega$ cm K^{-2}, yielding the Kadowaki–Woods ratio, $A/\gamma^2 \simeq 1.3(1) \times 10^{-6}$ $\mu\Omega$ cm (mol K $mJ^{-1})^2$. This figure is close to the theoretical predictions for d electrons by Rice [16], yielding $A/\gamma^2 \simeq 0.9 \times 10^{-6}$ $\mu\Omega$ cm (mol K $mJ^{-1})^2$ and also close to the generalized Kadowaki–Woods ratio of Kondo lattice systems yielding $A/\gamma^2 \sim 0.7 \times 10^{-6}$ $\mu\Omega$ cm (mol K $mJ^{-1})^2$ for sixfold degenerate Ce 4f moments [17].

Summing up, magnetic susceptibility and resistivity data suggest that the ordered stoichiometric compound $CeCo_9Si_4$ is a Kondo lattice on the verge of Co-ferromagnetism. The latter, however, is owing to the fact that this compound takes an exceptional position in the solid solution $CeCo_{9+\delta}Si_{4-\delta}$ where $CeCo_9Si_4$ is at the frontier between Si-richer and Co-richer sides where disorder occurs at different crystallographic sites of the space group $I4/mcm$.

4.2. Discussion

A direct comparison of the susceptibility and specific heat of stoichiometric $CeCo_9Si_4$ with earlier results regarding the itinerant electron metamagnet $LaCo_9Si_4$ [8] is shown in figures 8(a) and (b). While heat capacity data and, in particular, the linear coefficient of the electronic specific heat of $CeCo_9Si_4$ and $LaCo_9Si_4$ are almost alike (Sommerfeld coefficients γ near 200 mJ mol^{-1} K^{-2} in both cases), the corresponding paramagnetic susceptibilities, i.e. the extrapolated low temperature values $\chi(0)$ as well as the temperature dependences, $\chi(T)$, are rather different. While $LaCo_9Si_4$ with empty 4f orbitals exhibits a three times larger $\chi(2\text{ K}) \simeq 40 \times 10^{-3}$ emu mol^{-1} and a markedly temperature dependent susceptibility with a maximum at about 20 K, $CeCo_9Si_4$ with partly occupied 4f states shows evidence of a weakly temperature dependent susceptibility with $\chi(2\text{ K}) \simeq 17 \times 10^{-3}$ emu mol^{-1}. The presence of intermediate valent Ce obviously leads to a significant weakening of the ferromagnetic exchange coupling in the Co 3d bands and, thus, to a reduction of the Stoner enhancement of the d electron susceptibility as compared to $LaCo_9Si_4$. The latter reveals a Stoner enhancement factor of about 20 and almost fulfils the Stoner criterion for the onset of ferromagnetism [8].

The minor difference in the specific heat of $CeCo_9Si_4$ as compared to $LaCo_9Si_4$ is due to a compensation effect by a Kondo contribution from Ce. Earlier results of high-energy electron spectroscopy on $CeCo_9Si_4$ and $CeNi_9Si_4$ [10] indicate that the Kondo temperature $T_K \sim 400$ K of $CeCo_9Si_4$ is about four to five times larger than $T_K \sim 80$ K of $CeNi_9Si_4$, thus implying a 4f contribution to the Sommerfeld coefficient γ of about 20–30 mJ mol^{-1} K^{-2} for $CeCo_9Si_4$ and a contribution to the low temperature susceptibility $\chi(2\text{ K})$ of about (1–2) $\times 10^{-3}$ emu mol^{-1}. Accordingly, the Co 3d-subsystem contributes about 150 mJ mol^{-1} K^{-2} to γ, which is just modestly reduced when compared to $LaCo_9Si_4$. The weakening of the ferromagnetic exchange coupling in $CeCo_9Si_4$ obviously leads to a rather modest reduction of the spin-fluctuation mass enhancement of d electrons, which is about three in the case of $LaCo_9Si_4$.

The onset of weak ferromagnetism which is observed in both solid solutions, $CeCo_{9+\delta}Si_{4-\delta}$ and $LaCo_{9+\delta}Si_{4-\delta}$, for $\delta > 0$ is favoured by disorder at Si-16l sites and appears

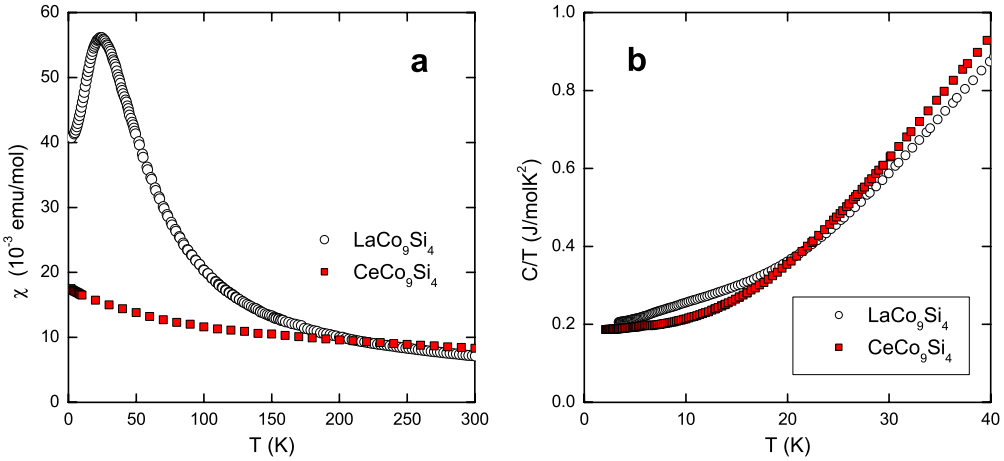

Figure 8. Comparison of the temperature dependent susceptibility (a) and specific heat (b) of $CeCo_9Si_4$ with $LaCo_9Si_4$ (data taken from [8]).

unrelated to the specific strength of ferromagnetic exchange in stoichiometric $CeCo_9Si_4$ or $LaCo_9Si_4$.

5. Conclusions

The investigation of the $CeCo_{13-x}Si_x$ system with nominal compositions varying from $CeCo_{10}Si_3$ to $CeCo_8Si_5$ by means of microprobe analysis and x-ray diffraction revealed the formation of the tetragonal $LaFe_9Si_4$ structure-type, essentially single phase samples $CeCo_{9+\delta}Si_{4-\delta}$ in a narrow composition range $-0.3 \leqslant \delta < 0.1$, where stoichiometric $CeCo_9Si_4$ exhibits a fully ordered arrangement of Ce, Co and Si atoms in the space group $I4/mcm$. Rietveld refinements performed on off-stoichiometric samples $CeCo_{8.7}Si_{4.3}$ and $CeCo_{9.4}Si_{3.6}$, indicate that excess Si (for $\delta < 0$) and excess Co atoms (for $\delta > 0$) with respect to the ordered compound $CeCo_9Si_4$ are not distributed randomly over the available crystallographic sites. On the one hand, excess Si shares the 16k site with Co, and on the other hand excess Co shares 16l sites with Si. The composition $CeCo_9Si_4$ is thus at the crossover between two kinds of disordered sublattices and, in fact, when proceeding along the solid solution through this point, magnetization measurements revealed the appearance of weak ferromagnetism on the Co-rich side ($\delta > 0$). These results compare rather well with earlier studies on the system $LaCo_{9+\delta}Si_{4-\delta}$, even though the presence of intermediate valence cerium in $CeCo_9Si_4$ clearly weakens the ferromagnetic exchange in the Co 3d-subsystem as compared to nearly ferromagnetic $LaCo_9Si_4$. The onset of weak ferromagnetism is thus attributed to substitutional disorder at Si-16l and it is not associated with any kind of a ferromagnetic critical point, neither in stoichiometric $CeCo_9Si_4$, which exhibits Kondo lattice features, nor in $LaCo_9Si_4$, which shows spin-fluctuation features of strongly exchange enhanced Pauli paramagnetism and a metamagnetic transition at moderately high magnetic fields.

Acknowledgment

The work was supported by the European Science Foundation under project Cost-P16, ECOM.

References

[1] Bodak O I 1979 *Sov. Phys.—Crystallogr.* **24** 732
[2] Tang W, Liang J, Chen X and Rao G 1994 *J. Appl. Phys.* **76** 4095
[3] Michor H, Berger S, El-Hagary M, Paul C, Bauer E, Hilscher G, Rogl P and Giester G 2003 *Phys. Rev.* B **67** 224428
Sengupta K and Sampathkumaran E V 2006 *J. Phys.: Condens. Matter* **18** L115
[4] Michor H, Bauer E, Dusek C, Hilscher G, Rogl P, Chevalier B, Etourneau J, Giester G, Killer U and Scheidt E-W 2004 *J. Magn. Magn. Mater.* **272–276** 227
[5] Killer U, Scheidt E-W, Eickerling G, Michor H, Sereni J, Pruschke T and Kehrein S 2004 *Phys. Rev. Lett.* **93** 216404
Peyker L, Gold C, Scheidt E-W, Scherer W, Donath J-G, Gegenwart P, Mayr F, Eyert V, Bauer E and Michor H 2009 *J. Phys.: Condens. Matter* **21** 235604
[6] Michor H, El-Hagary M, Özcan S, Horyn A, Bauer E, Reissner M, Hilscher G, Khmelevskyi S and Mohn P 2005 *Physica* B **359–363** 1177
[7] El-Hagary M, Michor H, Özcan S, Giovannini M, Matar A, Heiba Z, Kerschl P, Schönhart M, Bauer E, Grössinger R, Hilscher G, Freudenberger J and Rosner H 2006 *J. Phys.: Condens. Matter* **18** 4567
[8] Michor H, El-Hagary M, Della Mea M, Pieper M W, Reissner M, Hilscher G, Khmelevskyi S, Mohn P, Schneider G, Giester G and Rogl P 2004 *Phys. Rev.* B **69** 081404
[9] El-Hagary M, Michor H, Bauer E, Grössinger R, Kerschl P, Eckert D, Müller K-H, Rogl P, Giester G and Hilscher G 2005 *Physica* B **359–361** 311
[10] Wang X, Michor H and Grioni M 2007 *Phys. Rev.* B **75** 035127
[11] Rao G H, Liang J K, Zhang Y L, Cheng X R and Tang W H 1994 *Appl. Phys. Lett.* **64** 1650
[12] El-Hagary M, Michor H, Wind M, Bauer E, Hilscher G and Rogl P 2004 *J. Alloys Compounds* **367** 239
[13] Materials Preparation Center, Ames Laboratory, US DOE Basic Energy Sciences, Ames, IA, USA, available from: www.mpc.ameslab.gov
[14] Heiba Z K, El-Hagary M, Michor H and Hilscher G 2005 *Intermetallics* **14** 220
[15] Moze O, de Groot C H, de Boer F R and Buschow K H J 1996 *J. Alloys Compounds* **235** 62
[16] Rice M J 1968 *Phys. Rev. Lett.* **20** 1439
[17] Tsujii N, Kontani H and Yoshimura K 2005 *Phys. Rev. Lett.* **94** 057201